Available online at www.sciencedirect.com

ScienceDirect

IFAC Papers Online CONFERENCE PAPER ARCHIVE

IFAC PapersOnLine 59-37 (2025) 85–90

A General Identification Procedure for Reduced-Order Fractional Models Based on the Process Reaction Curve ⋆

Juan J. Gude *,1 **Antonio Di Teodoro** * **Oscar Camacho** **
Pablo García Bringas *

* *Faculty of Engineering, University of Deusto, 48007, Bizkaia, Bilbao, Spain.*
** *Colegio de Ciencias e Ingenierias, Universidad San Francisco de Quito, Quito 170157, Ecuador.*

Abstract: Recent advances in fractional calculus and computation have enabled the development of more accurate and flexible models for industrial process dynamics. Among these, the Fractional First-Order Plus Dead-Time (FFOPDT) and Fractional Dual-Pole Plus Dead-Time (FDPPDT) models have shown notable performance in representing systems with overdamped step responses. This work introduces a unified analytical identification procedure for both models, derived from the process reaction curve obtained through a simple open-loop step test. The proposed methodology is validated through numerical simulations, and the results demonstrate that it achieves comparable or superior performance to existing methods, with the added benefits of analytical simplicity and computational efficiency, making it suitable for industrial applications.

Keywords: Fractional systems, Process Identification, FFOPDT, FDPPDT, Reaction Curve.

1. INTRODUCTION

In industrial process control, accurate reduced-order models are essential for effective controller design, particularly for PID-based systems. Traditionally, this has been addressed using integer-order models such as the First-Order Plus Dead Time (FOPDT) and Second-Order Plus Dead Time (SOPDT) structures (Åström and Hägglund (2006)). However, such models often fall short when representing systems with long delays, memory effects, or anomalous diffusion, as commonly observed in thermal, chemical, and electrical systems (Sun et al. (2018); Petráš (2019)).

To address these limitations, fractional-order models have become increasingly popular due to their ability to describe system dynamics that lie between classical integer orders through non-integer derivatives (Almeida et al. (2016)). Among these, the Fractional First-Order Plus Dead-Time (FFOPDT) model is widely used for its balance between simplicity and accuracy. Several analytical identification techniques derived from the reaction curve have been proposed, including graphical, three-point, and generalized approaches (Tavakoli-Kakhki et al. (2010); Nie et al. (2016); Gude and García Bringas (2022b)).

Optimization-based techniques, such as those using the CRONE approach, PSO algorithms, or numerical fractional calculus, have shown high accuracy at the expense of increased computational cost (Alagoz et al. (2019); Guevara et al. (2015)). A recent hybrid approach balances accuracy and efficiency by combining optimization for α with analytical estimation of K, T, and L (Gude et al. (2024)).

More recently, the Fractional Dual-Pole Plus Dead-Time (FDPPDT) model has been introduced to extend the FFOPDT model's capability to represent overdamped or S-shaped responses in high-order fractional systems (Gude et al. (2025)). This model enhaces modeling accuracy by capturing more complex dynamics, and its identification relies exclusively on the analytical procedure presented in the same work, which uses reaction curve data.

This paper proposes a unified analytical identification approach for the FFOPDT and FDPPDT models, derived from the process reaction curve obtained through a simple open-loop step test. The technique uses only three arbitrary points, significantly reducing computational complexity and simplifying implementation. Simulation results confirm its accuracy compared to existing fractional-order identification techniques.

This paper is structured as follows: Section 2 introduces the mathematical background supporting the development of the proposed methodology. Section 3 details the general analytical identification procedure for both FFOPDT and FDPPDT models based on the reaction curve. Section 4 reports the simulation results that evaluate the accuracy of the suggested method in comparison with other benchmark techniques. Finally, Section 5 summarizes the main conclusions and outlines potential directions for future research.

⋆ This work was supported by the Basque Government (BEREZ-IA Elkartek Project, Grant KK-2023/00012) and by Universidad San Francisco de Quito (USFQ) through the Poli-Grants Program (Grant 33603).

[1] Corresponding author: jgude@deusto.es

10.1016/j.ifacol.2026.01.015

2. MATHEMATICAL BACKGROUND

2.1 Brief Introduction to Fractional Calculus

Definition 1. Let $\left(D^{\eta}_{a^+}h\right)(x)$ be the Riemann-Liouville fractional derivative of order $\eta \in \mathbb{R}$, $0 < \eta < 1$ (see Kilbas et al. (2006); Podlubny (1999); Samko et al. (1993)),

$$\left(D^{\eta}_{a^+}h\right)(x) = \frac{d}{dx}\,\frac{1}{\Gamma(1-\eta)}\int_a^x \frac{h(t)}{(x-t)^{\eta}}\,dt. \qquad (1)$$

where $[\eta]$ denotes the integer part of η, and Γ is the gamma function.

Definition 2. The Riemann–Liouville fractional integral of order $\eta > 0$ is defined as (see Kilbas et al. (2006); Podlubny (1999); Samko et al. (1993)):

$$\left(I^{\eta}_{a^+}h\right)(x) = \frac{1}{\Gamma(\eta)}\int_a^x \frac{h(t)}{(x-t)^{1-\eta}}\,dt, \quad x > a. \qquad (2)$$

We define the class $I^{\eta}_{a^+}(L_1)$ as the set of functions h that can be expressed as the fractional integral $h = I^{\eta}_{a^+}\varphi$, where φ is a summable function in the space $L_1(a,b)$. A comprehensive characterization of such functions can be found in (Kilbas et al. (2006); Samko et al. (1993)).

Theorem 3. A function $h \in I^{\eta}_{a^+}(L_1)$, with $\eta > 0$, if and only if $I^{p-\eta}_{a^+}h \in AC^p([a,b])$, where $p = [\eta] + 1$ and $(I^{p-\eta}_{a^+}h)^{(k)}(a) = 0$, for $k = 0, \ldots, p-1$.

Theorem 3 refers to $AC^s([a,b])$ as the set of functions h continuously differentiable up to order $s-1$, with an absolutely continuous $s-1$-th derivative on $[a,b]$. Dropping the absolute continuity condition broadens the class to include functions for which a summable fractional derivative exists.

Furthermore, as noted in (Podlubny, 1999, Sect. 2.3.6), fractional derivatives generally do not satisfy the semigroup property. This leads to the following result:

Lemma 4. Let $h \in AC^{p-1}([a,b])$ with $h^{(p)} \in L_1(a,b)$. Then, $D^{\eta}_{a^+}\left(D^{\gamma}_{a^+}h\right) = D^{\eta+\gamma}_{a^+}h$, provided that $h^{(j)}(a^+) = 0, \quad j = 0,1,\ldots,p-1$, where $p = [\gamma]+1$.

Remark 5. For simplicity in both calculations and implementation, we focus on the case $\eta \in (0,1)$. Nevertheless, the same reasoning can be extended to arbitrary intervals of η. Moreover, the fractional parameter $\eta_0 \in (0,1)$ may also be used in the Riemann–Liouville fractional derivative operator in equation (1), as $D^{\eta}_{+} = D^{\boldsymbol{\eta}}_{+} = D^{\frac{1+\eta_0}{2}}_{x_0^+}$.

Example 1. Let $\mu, \lambda \in (0,1)$, $a > 0$, $\mathrm{k} \in \mathbb{N}$ and $\beta > -1$, then

(1) $I^{\lambda}_{a}\left[(t-a)^{\beta}\right] = \frac{\Gamma(\beta+1)}{\Gamma(\beta+\lambda+1)}(t-a)^{\beta+\lambda}$.

(2) $D^{\mu}_{a}\left[(t-a)^{\beta}\right] = \begin{cases} 0, & \beta = \mu - 1, \\ \dfrac{\Gamma(\beta+1)}{\Gamma(\beta-\mu+1)}(t-a)^{\beta-\mu}, & \text{other } \beta. \end{cases}$

Remark 6. The Riemann–Liouville derivative of a constant is nonzero but recovers the expected behavior in the limit. Although it is related to the Caputo derivative, this connection is not addressed here, as we focus solely on the Riemann–Liouville formulation. Further details can be found in (Kilbas et al. (2006); Podlubny (1999); Samko et al. (1993)).

2.2 The Mittag-Leffler function: Derivative and integral

The two-parameter Mittag-Leffler function, as presented in (Samko et al. (1993); Rogosin (2015); Gorenflo et al. (2020)), is defined for all $z \in \mathbb{C}$ as follows:

$$E_{\alpha,\beta}(z) = \sum_{r=0}^{\infty}\frac{z^r}{\Gamma(\alpha r + \beta)}, \qquad (3)$$

$\alpha \in \mathbb{R}^+$, and $\beta \in \mathbb{C}$ (Podlubny (1999); Kilbas et al. (2006)). The function $E_{\alpha,\beta}$ generalizes the one-parameter Mittag-Leffler function, with the relation $E_{\alpha,1}(z) = E_{\alpha}(z)$. In particular, when $\alpha = 1$ and $\beta = 1$, the function reduces to the exponential function: $E_{1,1}(z) = E_1(z) = \exp(z)$. Hence, the Mittag-Leffler can be regarded as a natural extension of the exponential function (Rogosin (2015); Gorenflo et al. (2020)). Important results needed in this work concern the derivative and integral of the Mittag-Leffler function. Consider $\mu > 0$, $\lambda > 0$, and $\gamma \in \mathbb{C}$. Then:

$$\partial^{\mu}_{t_0^+}\left[t_1{}^{\mu-1}E_{\mu}(\gamma t_0{}^{\mu-1})\right] = \gamma t_1{}^{\mu-1}E_{\mu}(\gamma t_0{}^{\mu-1}), \qquad (4)$$

$$I^{\lambda}_{t_1^+}\left[t_1{}^{\mu-1}E_{\mu}(\gamma t_0{}^{\mu-1})\right] = \frac{\Gamma(\mu)}{\Gamma(\lambda+\mu)}t_1{}^{\mu+\lambda-1}E_{\mu}(\gamma t_0{}^{\mu-1}). \qquad (5)$$

To see some examples of how the Mittag-Leffler function is used to study asymptotic stability and applications in control theory, among others, see (Haubold et al. (2011); Gude et al. (2023)).

Remark 7. (Numerical version). It is important to highlight that the Grünwald–Letnikov derivative provides a discrete approximation of the Riemann–Liouville fractional derivative. This formulation is particularly suitable for numerical implementations, as it naturally lends itself to finite difference schemes. In the limit as the step size approaches zero, the Grünwald–Letnikov derivative converges to its continuous counterpart, thereby establishing a rigorous link between discrete and continuous fractional calculus.

2.3 Basic ordinary differential fractional equation solution

When the Laplace transform is applied to the Riemann–Liouville fractional derivative, the result is:

$$\mathscr{L}\{D^{\alpha}f(t)\} = s^{\alpha}F(s) - \sum_{k=0}^{n-1}s^{k}\left[D^{\alpha-k-1}f(t)\right]_{t=0^+}, \qquad (6)$$

where $n-1 \le \alpha < n$ and $F(s) = \mathscr{L}\{f(t)\}(s)$ denotes the Laplace transform of the function $f(t)$. The terms $\left[D^{\alpha-k-1}f(t)\right]_{t=0^+}$ represent the initial conditions involving fractional derivatives of $f(t)$ evaluated at $t = 0^+$. Assuming zero initial conditions, i.e., $\left[D^{\alpha-k-1}f(t)\right]_{t=0^+} = 0$ for all $k = 0,1,\ldots,n-1$, the expression simplifies to: $\mathscr{L}\{D^{\alpha}f(t)\} = s^{\alpha}\mathscr{L}\{f(t)\}$. This is analogous to the classical property of integer-order derivatives in the Laplace domain, where differentiation in time corresponds to multiplication by s. To examine the role of initial conditions more closely, consider the following equation:

$$D^{2\alpha}y_{\alpha}(t) + D^{\alpha}y_{\alpha}(t) + y_{\alpha}(t) = t^{\alpha-1}Ku(t-L). \qquad (7)$$

Note that, due to the definition of the Riemann–Liouville derivative, enforcing initial conditions at $t = 0$ is mathematically challenging, except in trivial cases or when

considering asymptotic behavior. To illustrate this briefly, for $a = 0$, a trivial solution of equation (7) is:

$$y_\alpha(t) = \frac{Ku(t-L)}{\Gamma(\alpha)\,\Gamma((m+1)\,\alpha)}t^{\alpha-1} \tag{8}$$

which satisfies the initial condition under certain assumptions. Another possible solution is given by:

$$y_\alpha(t) = Ct^{\alpha-1}Ku(t-L) + f(\eta)E_\alpha(t^\alpha) \tag{9}$$

where $f(\eta) = \eta^2 + \eta + \epsilon$. This solution satisfies the initial condition only asymptotically; in general,

$$\left|\left[D^{\alpha-k-1}f(t)\right]_{t=0^+}\right| = \epsilon > 0. \tag{10}$$

for all $k = 0, 1, \ldots, n-1$, where ϵ is a small quantity.

Consequently, $\lim_{\epsilon\to 0}\left|\left[D^{\alpha-k-1}f(t)\right]_{t=0^+}\right| \to 0$

Remark 8. We are aware of the ongoing discussion regarding the proper treatment of initial conditions in fractional calculus. Current research efforts, such as those involving weighted fractional operators (Fernandez and Fahad (2022); Contreras et al. (2025); Katugampola (2011)), aim to address these issues. However, for the purposes of this work, we consider natural modifications of the solution in (9) that asymptotically tend to zero, thereby satisfying the initial conditions in the required sense.

2.4 The models under consideration

The FFOPDT model provides a simple yet effective representation of fractional process dynamics. Its differential equation is:

$$TD^\alpha y_\alpha(t) + y_\alpha(t) = Ku(t-L). \tag{11}$$

To describe higher-order fractional dynamics exhibiting overdamped or S-shaped step responses, the FDPPDT model is employed. Its differential equation is:

$$T^2D^{2\alpha}y_\alpha(t) + 2TD^\alpha y_\alpha(t) + y_\alpha(t) = Ku(t-L). \tag{12}$$

Assuming zero initial conditions, $\left[D^{\alpha-k-1}y_\alpha(t)\right]_{t=0^+} = 0$ for all $k = 0, 1, \ldots, n-1$, or equivalently when deviation variables are used, the transfer functions of both models can be derived as follows. For the FFOPDT model:

$$P(s) = \frac{Y_\alpha(s)}{U(s)} = \frac{\mathscr{L}\{y_\alpha(t)\}}{\mathscr{L}\{u(t)\}} = \frac{Ke^{-Ls}}{1+Ts^\alpha}, \tag{13}$$

and for the FDPPDT model:

$$P(s) = \frac{Y_\alpha(s)}{U(s)} = \frac{\mathscr{L}\{y_\alpha(t)\}}{\mathscr{L}\{u(t)\}} = \frac{Ke^{-Ls}}{(1+Ts^\alpha)^2}. \tag{14}$$

In equations (11) and (12), $y_\alpha(t)$ denotes the process output and $u(t)$ the process input, with D^α representing the Riemann–Liouville fractional derivative operator. In the corresponding transfer functions (13) and (14), K is the process gain, T the time constant, L the dead time, and α the fractional order. It is assumed that $T > 0$ and $L \geq 0$. Furthermore, in both cases it is assumed that the initial conditions are satisfied and asymptotically tend to zero, that is, $\lim_{\epsilon\to 0}\left|\left[D^{\alpha-k-1}y_\alpha(t)\right]_{t=0^+}\right| \to 0$

Remark 9. A discussion on commensurability and its description using rational functions of polynomial type can be found in (Aboukheir et al. (2024); Gude et al. (2024)).

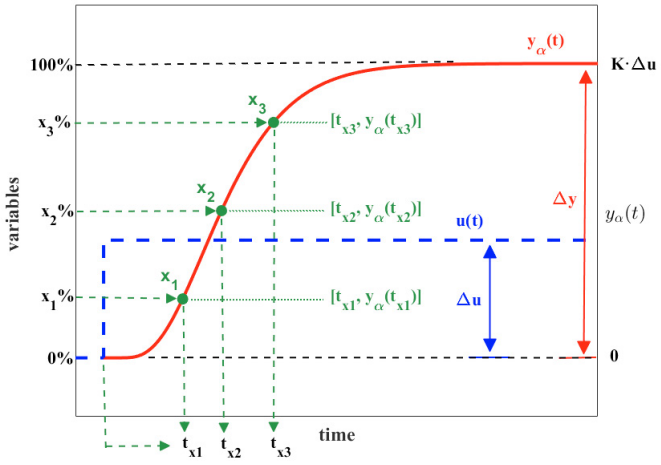

Fig. 1. Typical reaction curve $y_\alpha(t)$ and input $u(t)$, showing the characteristic overdamped fractional response described by FFOPDT or FDPPDT models with key data highlighted for parameter estimation.

3. GENERAL ANALYTICAL IDENTIFICATION PROCEDURE FOR FFOPDT AND FDPPDT MODELS

This section presents a unified procedure to identify FFOPDT and FDPPDT models using open-loop step response data. The approach builds upon the methods introduced in (Gude and García Bringas (2022b)) for FFOPDT and (Gude et al. (2025) for FDPPDT, providing a common framework applicable to both formulations.

This procedure is suitable for processes with S-shaped step responses and effectively models this fractional-order behavior using either FFOPDT or FDPPDT formulations. Figure 1 illustrates the process reaction curve along with the quantities required to extract the parameters of the models.

The time-domain step responses of the FFOPDT (13) and FDPPDT (14) models corresponding to a step input of amplitude Δu are given by:

$$y_\alpha(t) = K\Delta u\left\{1 - E_\alpha\left[-\frac{1}{T}(t-L)^\alpha\right]\right\}, \tag{15}$$

$$y_\alpha(t) = K\Delta u\left\{1 - \left(1 + \frac{(t-L)^\alpha}{T}\right)E_\alpha\left[-\frac{1}{T}(t-L)^\alpha\right]\right\}, \tag{16}$$

where K, T, L, and α are model parameters, E_α is the one-parameter Mittag-Leffler function (Podlubny (1999)), and $\Delta y = K \cdot \Delta u$ is the steady-state process output variation.

For $\alpha = 1$, (15) reduces to the classical FOPDT model, and (16) becomes the standard DPPDT model.

Normalizing the output by Δy and introducing the dimensionless time variable $\tau = \frac{(t-L)^\alpha}{T}$, the step responses (15) and (16) become:

$$\tilde{y}_\alpha(\tau) = \frac{y_\alpha(\tau)}{\Delta y} = 1 - E_\alpha(\tau), \tag{17}$$

$$\tilde{y}_\alpha(\tau) = \frac{y_\alpha(\tau)}{\Delta y} = 1 - (1+\tau)E_\alpha(-\tau) \tag{18}$$

where $\tilde{y}_\alpha(\tau)$ is the normalized output of both models in terms of the dimensionless time τ.

The proposed identification procedure requires three points from the step process response. Let t_x denote the time at which the process output reaches $x\%$ of its total variation ($x \in [0, 100]$), as shown in Figure 1, and τ_x the corresponding normalized time for the normalized output $\tilde{y}_\alpha(\tau_x) \in [0, 1]$. The sets $\{t_{x1}, t_{x2}, t_{x3}\}$ and $\{\tau_{x1}, \tau_{x2}, \tau_{x3}\}$ are computed from equations (15) and (17) for FFOPDT, and (16) and (18) for FDPPDT models, respectively.

The parameters of both models are estimated as follows (see Gude and García Bringas (2022b); Gude et al. (2025)):

$$\begin{cases} K = \dfrac{\Delta y}{\Delta u}, \\ \alpha = f_1(\Delta), \\ T = f_2(\alpha) \cdot (t_{x3} - t_{x1})^\alpha, \\ L = \max\left[t_{x3} - f_3(\alpha) \cdot T^{1/\alpha},\ 0\right] \end{cases} \tag{19}$$

where $\{\Delta y, \Delta u, t_{x1}, t_{x2}, t_{x3}\}$ are obtained from the process reaction curve. The functions $f_1(\Delta)$, $f_2(\alpha)$, and $f_3(\alpha)$ are fitted expressions (e.g., polynomial, exponential, or rational) derived from the data sets $\{\alpha,\ \Delta\}$, $\{a^\alpha,\ \alpha\}$, and $\{\tau_{x3}^{1/\alpha},\ \alpha\}$, respectively, for $\alpha \in [0.5, 1.0]$, where $a = \frac{1}{\tau_{x3}^{1/\alpha} - \tau_{x1}^{1/\alpha}}$ and $\Delta = \frac{\tau_{x3}^{1/\alpha} - \tau_{x1}^{1/\alpha}}{\tau_{x2}^{1/\alpha} - \tau_{x1}^{1/\alpha}} = \frac{t_{x3} - t_{x1}}{t_{x2} - t_{x1}}$.

Figure 2 presents the unified FFOPDT/FDPPDT identification procedure, which fits three points (x_1–x_2–x_3%) on the reaction curve and is organized into two main parts:

Part A (blue) outlines the derivation of the functions $f_1(\Delta)$, $f_2(\alpha)$, and $f_3(\alpha)$, which depend on the model type (FFOPDT or FDPPDT), the selected points $\{x_1, x_2, x_3\%\}$, the normalized times τ_{x1}, τ_{x2}, and τ_{x3}, and the fitting technique. These functions are constructed from the normalized step responses (17) and (18), typically in advance to enable parameter estimation using equations (19).

Part B (red) illustrates the identification algorithm itself. It uses the fitted functions and the data set $\{\Delta y, \Delta u, t_{x1}, t_{x2}, t_{x3}\}$, extracted from a simple open-loop test, to identify the model parameters.

4. SIMULATION RESULTS

4.1 Experimental procedure

In this section, we validate the proposed unified identification method for FFOPDT and FDPPDT models through its application to a high-order fractional process, comparing the derived reduced-order models with previously reported analytical and optimization-based approaches.

For illustrative purposes, the set $x_1 = 10\%$, $x_2 = 50\%$, and $x_3 = 90\%$ is used, though the method is general and applicable to any arbitrary set (x_1–x_2–x_3%) (Gude and García Bringas (2025)).

The functions f_1, f_2, and f_3 for both models are fitted over $0.50 \leq \alpha \leq 1.00$, using data sets $\{\Delta, \alpha\}$, $\{\alpha, f_2\}$, and $\{\alpha, f_3\}$, and using the Levenberg-Marquardt least-squares algorithm.

A common rational function is used for both models:

$$f_k(x) = \frac{\sum_{i=1}^{n_k} p_i x^i}{\sum_{j=1}^{m_k} q_j x^j}, \tag{20}$$

where $k \in \{1, 2, 3\}$, x represents Δ for $k = 1$ and α for $k = 2, 3$, n_k and m_k denote the degrees of the numerator and denominator polynomials, respectively, and p_i and q_j are real coefficients.

The fitted coefficients $\{p_i, q_i\}$ are provided in Tables 1 and 2 for FFOPDT and FDPPDT models, respectively.

Table 1. Parameters of the rational functions f_k ($k = 1, 2, 3$) for FFOPDT models.

$f_1(\Delta)$	$f_2(\alpha)$	$f_3(\alpha)$
$p_1 = 0.3854$	$p_1 = -0.0673$	$p_1 = 4.066$
$p_2 = 12.75$	$p_2 = 0.1578$	$p_2 = -7.705$
$p_3 = -3.517$	–	$p_3 = 5.055$
$q_1 = 13.5$	$q_1 = -2.501$	$q_1 = -0.4136$
$q_2 = -14.93$	$q_2 = 1.699$	$q_2 = 0.02868$

Table 2. Parameters of the rational functions f_k ($k = 1, 2, 3$) for FDPPDT models.

$f_1(\Delta)$	$f_2(\alpha)$	$f_3(\alpha)$
$p_1 = 0.3736$	$p_1 = -0.0487$	$p_1 = 6.79 \cdot 10^4$
$p_2 = 9.9695$	$p_2 = 0.0613$	$p_2 = -1.40 \cdot 10^5$
$p_3 = -6.6376$	–	$p_3 = 8.70 \cdot 10^4$
$q_1 = 9.2318$	$q_1 = -2.2501$	$q_1 = 8.93 \cdot 10^3$
$q_2 = -10.6337$	$q_2 = 1.2926$	$q_2 = -6.01 \cdot 10^3$
–	–	$q_3 = 1.05 \cdot 10^3$

4.2 Simulation Example

In this example, the process is represented by the following transfer function:

$$P(s) = \frac{K}{(1 + Ts^\lambda)^n} \tag{21}$$

where $K = 2$, $T = 1$ s, $n = 5$, and $\lambda = 0.85$. This model, originally introduced in (Tavakoli-Kakhki et al. (2010)), exhibits fractional-order dynamics characterized by the presence of repeated fractional poles.

An open-loop step test provides the following experimental data, required to apply the proposed identification procedure: $\Delta u = 1.00$, $\Delta y = 2.00$, $t_{10} = 2.35$ s, $t_{50} = 5.85$ s, and $t_{90} = 19.20$ s.

The estimated parameters are:
FDPPDT: $K = 2.00$, $T = 2.20$ s, $L = 1.39$ s, $\alpha = 0.855$;
FFOPDT: $K = 2.00$, $T = 5.07$ s, $L = 1.89$ s, $\alpha = 0.912$.

For the example under consideration, the close agreement between the estimated parameters and those obtained in (Gude et al. (2025)) and (Gude and García Bringas (2025)) confirms that the unified procedure preserves the accuracy of the individual identification approaches.

Figures 3 and 4 show the step responses of the identified models, computed from $N_S = 3\,001$ samples, with mean square error (MSE) values of $S_{FDPPDT} = 5.30 \times 10^{-5}$ and $S_{FFOPDT} = 3.81 \times 10^{-4}$, confirming that both models accurately reproduce the experimental behavior.

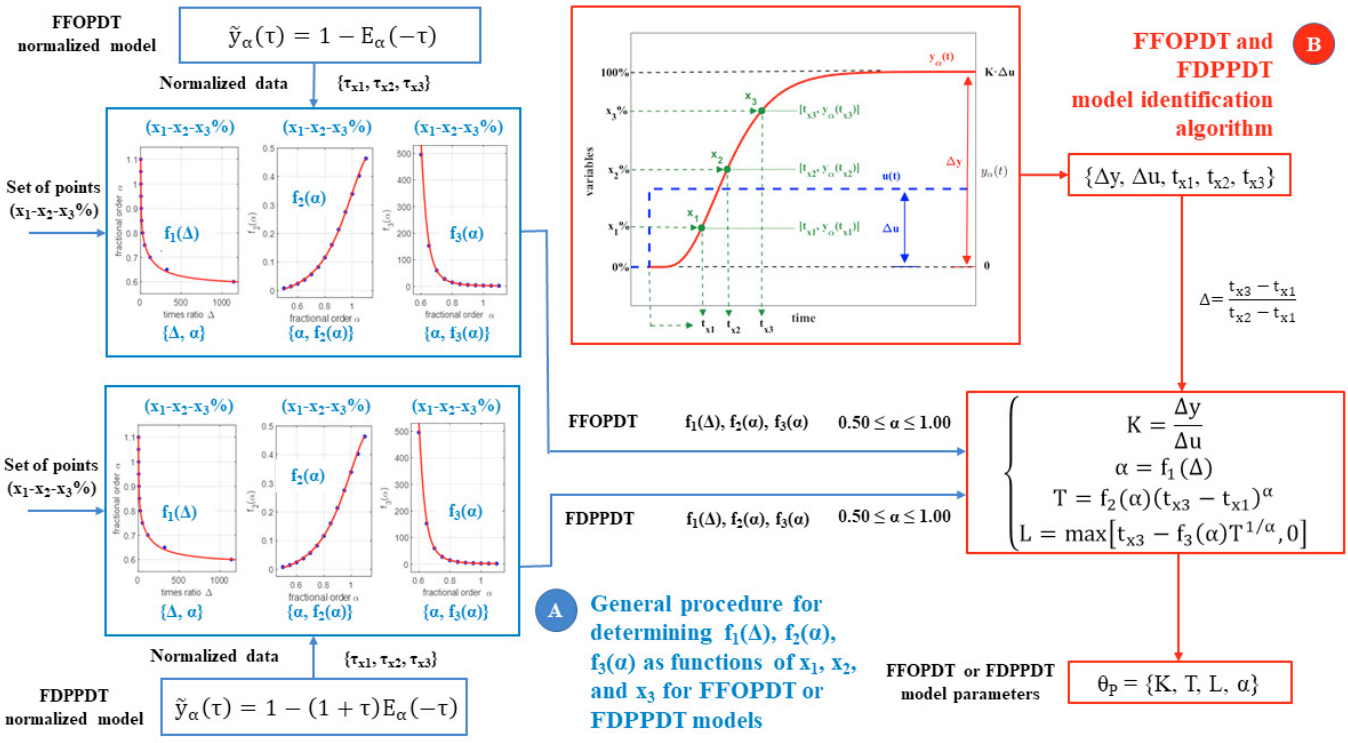

Fig. 2. Complete diagram of the common identification technique for FFOPDT and FDPPDT models.

These results confirm that a unified methodology can be effectively applied to identify the parameters of FFOPDT and FDPPDT models in a straightforward and consistent manner. For interested readers, (Gude et al. (2025)) provides a detailed comparison of the FDPPDT model identification method with other reaction-curve-based approaches for FFOPDT models, highlighting its superior capability to represent higher-order fractional dynamics. Furthermore, the proposed procedure provides a unified framework for determining, using a single method, whether the FDPPDT or FFOPDT model offers a more accurate representation of the process dynamics under study.

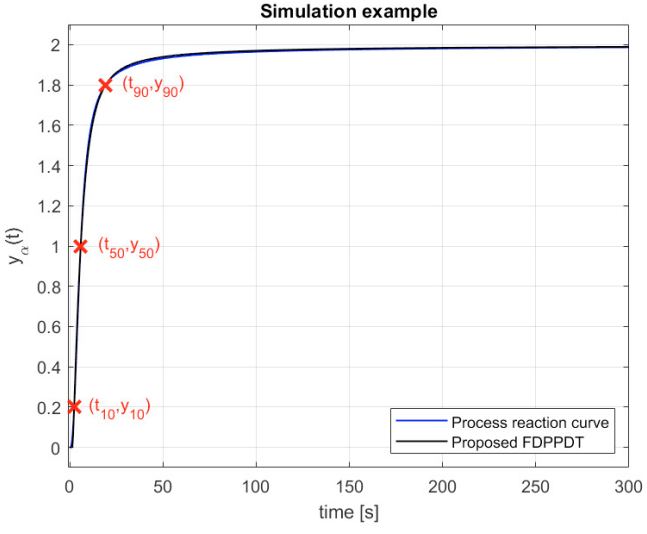

Fig. 3. Reaction curve and step response of the FDPPDT model estimated with the proposed technique.

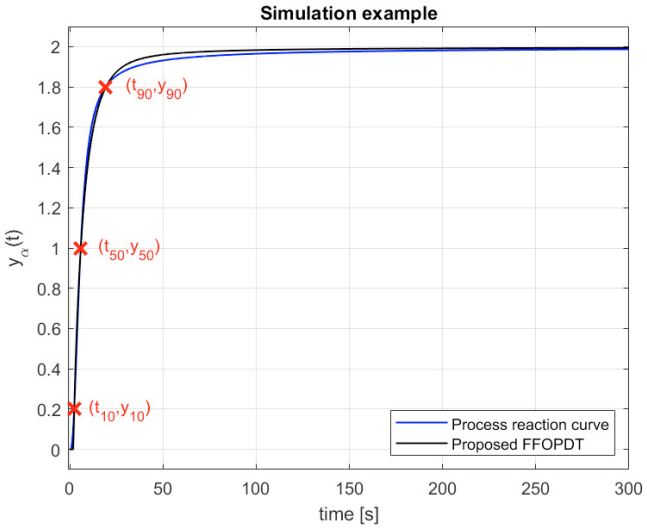

Fig. 4. Reaction curve and step response of the FFOPDT model estimated with the proposed technique.

4.3 Practical and experimental considerations

Due to space limitations, only simulation results are presented in this paper. However, several works have demonstrated the application of fractional-order model identification methods on experimental prototypes. Specifically, (Gude and García Bringas (2022a)) proposed a novel control hardware architecture enabling the implementation of fractional-order identification and control algorithms. Additional examples of analytical identification methods for FFOPDT models applied to experimental setups can be found, e.g., in Gude and García Bringas (2022b); Gude et al. (2023); Nie et al. (2016). Similarly, Gude et al. (2025)

reports the experimental validation of both FFOPDT and FDPPDT identification methods using a temperature-based laboratory prototype.

In industrial environments, measurement noise often affects the feedback signal of the controlled process. When such noisy signals are used for model identification or control, appropriate filtering becomes necessary. Nevertheless, since filter dynamics inherently modify the overall process response, the proposed identification procedure does not explicit account for the effects of measurement noise. Future work will therefore address the influence of filtering and noise on parameter estimation accuracy and model reliability under real operating conditions.

5. CONCLUSIONS

This work has presented a unified analytical procedure for identifying fractional-order reduced models (FFOPDT and FDPPDT) using simple data from the process reaction curve. The unified methodology provides closed-form analytical expressions for parameter estimation.

The proposed approach provides high modeling accuracy for overdamped systems with low computational cost, making it suitable for real-time or embedded control. Simulations show that the identified models match or outperform existing analytical and optimization-based methods. Its flexibility to adapt to different point sets broadens its applicability, supporting further advances in fractional control and industrial implementation.

REFERENCES

Aboukheir, H., Romero, J., and Di Teodoro, A. (2024). An approach for fractional commensurate order youla parametrization using q-weighted operator. In *Proceedings of the 21st International Conference on Informatics in Control, Automation and Robotics - Volume 1: ICINCO*, 706–713. INSTICC, SciTePress. doi:10.5220/0013058700003822.

Alagoz, B.B., Tepljakov, A., Ates, A., Petlenkov, E., and Yeroglu, C. (2019). Time-domain identification of one noninteger order plus time delay models from step response measurements. *International Journal of Modeling, Simulation, and Scientific Computing*, 10(01), 1941011.

Almeida, R., Bastos, N.R., and Monteiro, M.T.T. (2016). Modeling some real phenomena by fractional differential equations. *Mathematical Methods in the Applied Sciences*, 39(16), 4846–4855.

Åström, K.J. and Hägglund, T. (2006). *Advanced PID control*. ISA-The Instrumentation, Systems and Automation Society.

Contreras, E., Di Teodoro, A., and Mena, M. (2025). Fractional einstein field equations in $2+1$ dimensional spacetime. *General Relativity and Gravitation*, 57(5), 1–21.

Fernandez, A. and Fahad, H.M. (2022). Weighted fractional calculus: a general class of operators. *Fractal and Fractional*, 6(4), 208.

Gorenflo, R., Kilbas, A.A., Mainardi, F., Rogosin, S.V., et al. (2020). *Mittag-Leffler functions, related topics and applications*. Springer.

Gude, J.J., Camacho, O., Di Teodoro, A., and García Bringas, P. (2025). Analytical method for the identification of higher-order fractional systems using fractional dual-pole plus dead-time models. *Results in Engineering*, 105574.

Gude, J.J., Di Teodoro, A., Camacho, O., and García Bringas, P. (2023). A new fractional reduced-order model-inspired system identification method for dynamical systems. *IEEE Access*, 11, 103214–103231.

Gude, J.J. and García Bringas, P. (2022a). A novel control hardware architecture for implementation of fractional-order identification and control algorithms applied to a temperature prototype. *Mathematics*, 11(1), 143.

Gude, J.J. and García Bringas, P. (2022b). Proposal of a general identification method for fractional-order processes based on the process reaction curve. *Fractal and Fractional*, 6(9), 526.

Gude, J.J. and García Bringas, P. (2025). Improving a reaction curve-based analytical identification technique for fractional models. *International Journal of Dynamics and Control*, 13(3), 106.

Gude, J.J., García Bringas, P., Herrera, M., Rincón, L., Di Teodoro, A., and Camacho, O. (2024). Fractional-order model identification based on the process reaction curve: A unified framework for chemical processes. *Results in Engineering*, 21, 101757.

Guevara, E., Meneses, H., Arrieta, O., Vilanova, R., Visioli, A., and Padula, F. (2015). Fractional order model identification: Computational optimization. In *2015 IEEE 20th Conference on Emerging Technologies & Factory Automation (ETFA)*, 1–4. IEEE.

Haubold, H.J., Mathai, A.M., and Saxena, R.K. (2011). Mittag-leffler functions and their applications. *Journal of applied mathematics*, 2011(1), 298628.

Katugampola, U.N. (2011). A new approach to generalized fractional derivatives. *arXiv preprint arXiv:1106.0965*.

Kilbas, A., Srivastava, H., and Trujillo, J. (2006). *Theory and Applications of Fractional Differential Equations*, volume 204 of *North-Holland Mathematics Studies*. Elsevier, Amsterdam.

Nie, Z., Wang, Q., Liu, R., and Lan, Y. (2016). Identification and pid control for a class of delay fractional-order systems. *IEEE/CAA Journal of Automatica Sinica*, 3(4), 463–476.

Petráš, I. (2019). *Handbook of Fractional Calculus with Applications*. De Gruyter.

Podlubny, I. (1999). *Fractional Differential Equations*. Academic Press, San Diego.

Rogosin, S. (2015). The role of the mittag-leffler function in fractional modeling. *Mathematics*, 3(2), 368–381.

Samko, S., Kilbas, A., and Marichev, O. (1993). *Fractional Integrals and Derivatives: Theory and Applications*. Gordon and Breach, Yverdon.

Sun, H., Zhang, Y., Baleanu, D., Chen, W., and Chen, Y. (2018). A new collection of real world applications of fractional calculus in science and engineering. *Communications in Nonlinear Science and Numerical Simulation*, 64, 213–231.

Tavakoli-Kakhki, M., Haeri, M., and Tavazoei, M.S. (2010). Simple fractional order model structures and their applications in control system design. *European Journal of Control*, 16(6), 680–694.